ChemComm

Accepted Manuscript

This article can be cited before page numbers have been issued, to do this please use: S. Yang, Q. Sun, H. Xiong, S. Liu, B. Moosavi, W. Yang and G. Yang, *Chem. Commun.*, 2017, DOI: 10.1039/C7CC00577F.

ROYAL SOCIETY OF CHEMISTRY

rsc.li/chemcomm

ChemComm

View Article Online
DOI: 10.1039/C7CC00577F

COMMUNICATION

Discovery of A Butyrylcholinesterase-specific Probe via Structure-based Design Strategy

Received 00th January 20xx,
Accepted 00th January 20xx

DOI: 10.1039/x0xx00000x

www.rsc.org/

Shu-Hou Yang,[ac] Qi Sun,[ac] Hao Xiong,[a] Shi-Yu Liu,[a] Behrooz Moosavi,[a] Wen-Chao Yang,[a]* and Guang-Fu Yang[ab]*

We report herein the structure-based design and application of a fluorogenic molecular probe (BChE-FP) specific to butyrylcholinesterase (BChE). This probe was rationally designed by mimicking the native substrate and optimized stepwise by manipulating the steric feature and the reactivity of the designed probe targeting the structural difference of the active pocket of BChE and AChE. The refined probe, BChE-FP, exhibits a high specificity toward BChE compared to AChE, producing about 275-fold higher fluorescence enhancement upon the catalysis by BChE. Thus, BChE-FP is a specific BChE probe identified by structure-based design and it can discriminate BChE from AChE. Furthermore, it has been successfully applied for imaging the endogenous BChE in living cells, as well as the BChE inhibitor screening and characterization under physiological conditions.

Acetylcholinesterase (AChE; EC 3. 1.1.7) and butyrylcholinesterase (BChE; EC 3. 1.1.8) are two major human esterases and the focus of rigorous studies in pharmacology and neurobiology, due to their significant roles in human physiology and health.[1] The BChE have been implicated in lipid metabolism and various human diseases such as liver damage, diabetes, Alzheimer's disease (AD) and liver metastasis.[2] BChE is also responsible for detoxifying xenobiotics such as organophosphates and cocaine, and its engineered mutants have drawn a great deal of interest as detoxifying therapeutics.[3] Thus, the quantification of BChE activity and its inhibition are highly important in drug discovery and clinical diagnostics.

To date, four major methods have been developed for assessment of the activity of cholinesterases as follows: 1) UV/Vis assays with direct chromogenic reaction catalyzed by cholinesterases, or the direct product which could be further converted into a colored product with a thiol-capping agent such as Ellman's reagent (5,5'-dithiobis-(2-nitrobenzoic acid), DTNB); 2) fluorometric assays with fluorogenic substrates or indirect detection that yields fluorescence enhancement; 3) radiometric assays with ^{14}C or ^{3}H labeled substrates such as acetylcholine; 4) calorimetric assays with natural substrates by isothermal titration calorimetry.[4] The radiometric and calorimetric methods are accurate and are based on direct measurement, but not suitable for high-throughput analysis; the common UV/Vis and fluorometric methods are fast, sensitive and compatible with high-throughput experiments, but both mainly utilize a second reaction to generate the optical signal. Recently, extensive studies have been carried out to develop new fluorescent probes for assessment of the cholinesterases activity, but only in few of them fluorophore-based probes were developed for direct cholinesterases activity evaluation in a one-step reaction.[5] Most importantly, very few reported fluorescent probe[6] could discriminate BChE from AChE, due to the substantially similar biochemical properties of both cholinesterases. Therefore, development of a sensitive and specific probe for assessment of BChE activity and inhibitors screening is highly desirable; a crucial issue that we sought to solve in the current study.

We analyzed the catalytical mechanism[7] especially the difference on the active sites of BChE (PDB entry: 1P0M) and AChE (PDB entry: 1B41) (Fig. 1)[8]. Inspired by the previous studies on the development of fluorogenic probes targeting the esterases *in vitro* and *in vivo*,[9] we designed the probes (Fig. 2) by mimicking the native substrate and optimized stepwise by manipulating the steric feature and the reactivity of the designed probes targeting the structural difference of the active pockets of BChE and AChE. After optimization and comprehensive characterization, the refined BChE probe (termed as **BChE-FP**) showed good properties as follows: 1) it exhibits good specificity and could discriminate BChE from AChE; 2) about 275-fold fluorescence intensity (FI) enhancement in pure aqueous solution; and 3) about 100-fold higher binding affinity against BChE and comparable catalytic

[a] Key Laboratory of Pesticide and Chemical Biology, Ministry of Education, College of Chemistry, Central China Normal University, Wuhan 430079, P. R. China. E-mail: tomyang@mail.ccnu.edu.cn, gfyang@mail.ccnu.edu.cn
[b] Collaborative Innovation Center of Chemical Science and Engineering, Tianjin 30071, P.R. China.
[c] They contributed equally to this work.
†Electronic Supplementary Information (ESI) available: experiment section, UV-Vis absorption, fluorescence emission, theoretical calculation, ^{1}H NMR, ^{13}C NMR and MS spectra of all the new compounds were available in Supporting Information. See DOI: 10.1039/x0xx00000x

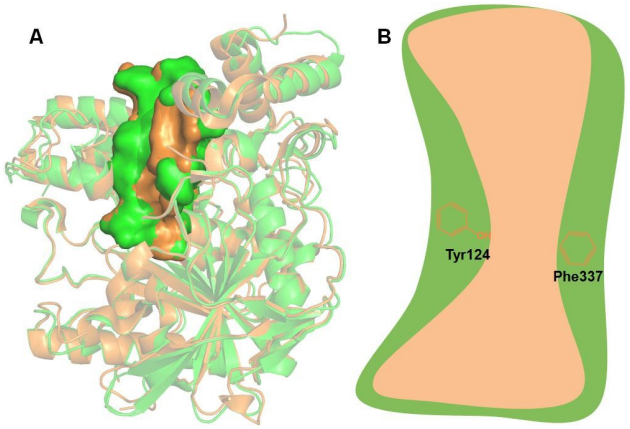

Fig. 1. (A) Superposition of the crystal structures of human BChE (green) and AChE (orange), their active sites were displayed in surface format. (B) The sectional view of active sites for BChE (green) and AChE (orange). Two aromatic residues (Tyr124 and Phe337) locating in the middle of AChE active site were indicated, respectively.

efficiency when comparing with the widely used substrate acetylthiocholine Iodide (ATC).

Starting from the natural substrate, butyrylcholine, the butyryl group was retained, and several fluorophores with different bulky size were introduced to construct the first series of probes **I1**-**5** in Fig. 2. All the probes of this series were fully characterized (See Schemes S1-S5 and Fig. S1-S9). The time-dependent FI changes of each reaction system, defined as the relative reaction rates (ΔF/Δt), were measured and listed in Table S1, applying the most wildly used natural substrate analog acetylthiocholine (ATC) as a reference. The screening results indicated that FI enhancement of probe **I5** was about 250-fold for BChE detection. This result suggests that carboxyfluorescein is the preferred fluorophore for BChE probe design. Therefore, we reserved the carboxyfluorescein and built the second set of probes to further optimize the butyryl group of probe **I5**. Considering the structural diversity of recognition group having different steric effect, various substituents were utilized to establish the second series of probes (**II1**-**10**, Scheme S5 and Fig. S10-S29), including short chain alkyl and cycloalkyl substituents. Based on the screening results in Fig. S30 and Table S1, probe **II4** with the highest relative reaction rates and about 14.5-fold selectivity, termed as **BChE-FP**, was finally chosen for the following studies.

The pH profile of the hydrolysis of **BChE-FP** catalyzed by BChE was firstly investigated, and the relative reaction rate (ΔF/Δt) was accelerated by increasing the pH ranging from 4.5 to 9.0 (See Fig S31-32). Considering that the physiological condition is neutral, the primary study was carried out at pH 7.0. Under this neutral pH, the time-dependence of the FI enhancement for **BChE-FP** was observed upon the addition of BChE, and the maximum FI at 515 nm indicated around 275-fold increase over the basal level (Fig. 3A). The data showed that **BChE-FP** could be considered a sensitive fluorescence "off-on" system for sensing BChE activity. In addition, the reaction mixture (100 mM phosphate buffer, 20 μM **BChE-FP**

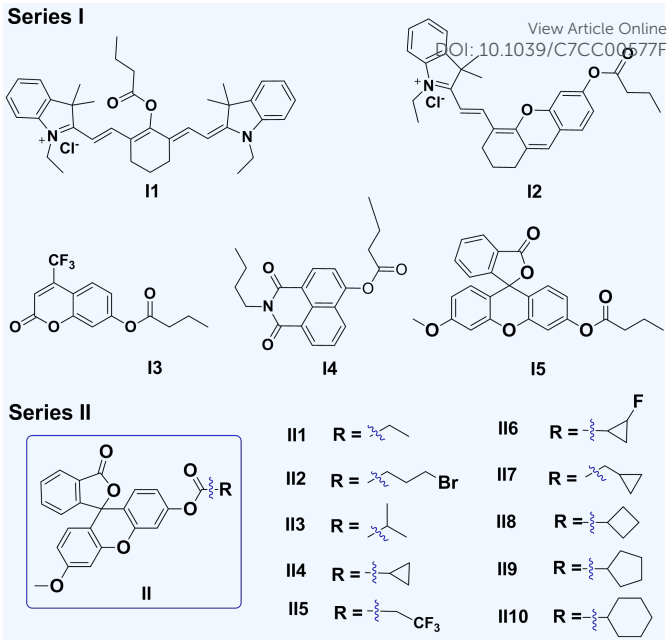

Fig. 2 Chemical structures of the designed probes, series **I** and **II**.

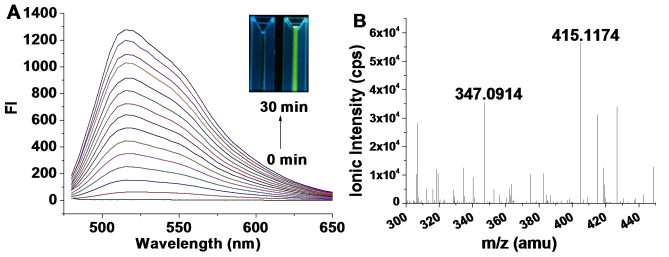

Fig. 3 (A) The time-dependent fluorescence (λ_{ex} = 455 nm) of **BChE-FP** (10 μM) in phosphate buffer (100 mM, pH 7.0) in the presence of BChE (0.02 U/mL) at 30 °C; Inset shows the photos of the corresponding reaction mixture in the absence and presence of BChE after 30 min incubation at 30 °C under UV light (365 nm) illumination. (B) HRMS spectrum of **BChE-FP** (20 μM) incubated with BChE (0.02 U/mL) for 30 min in the same buffer at 30 °C.

and 0.02 U/mL BChE) was analyzed by both HRMS (Fig. 3B) and HPLC (Fig. S33) methods, with similar reaction system containing no BChE as the negative control, which indicated that the fluorescence enhancement was the result of BChE-catalyzed hydrolysis of **BChE-FP** at the ester bond.

To uncover the specificity of this refined probe, the hydrolysis of **BChE-FP** was examined under the same conditions in the presence of various analytes, including metal ions (K^+, Na^+, Mg^{2+}, Ca^{2+}, Mn^{2+}), amino acids and biothiols (Arg, GSH, Phe, His). The data presented in Fig. S34 shows that this molecular probe is highly selective for BChE over competing amino acids, metal ions, and thiols. We also tested the reactivity of **BChE-FP** with other common enzymes or proteins (elastase, AChE, BChE, trypsin, chymotrypsin, phospholipase, alkaline phosphatase (ALP) and BSA). The results are summarized in Fig 4. We also tried the specificity study in Krebs buffer and no obvious interference was observed. It clearly demonstrated the relative reaction rate of BChE-

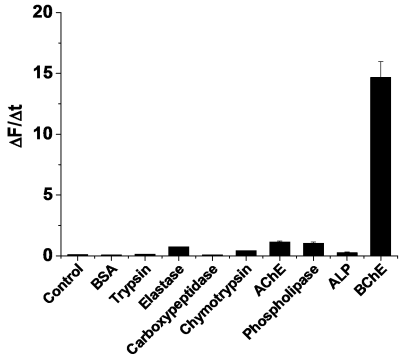

Fig. 4 The specificity profile of **BChE-FP** (10 μM) toward different hydrolases or proteins (elastase, AChE, BChE, trypsin, BSA, phospholipase, ALP and chymotrypsin).

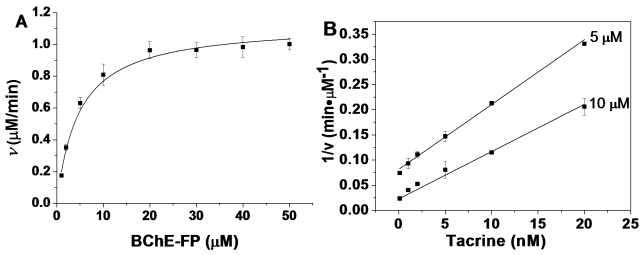

Fig. 5 (A) Michaelis-Menten curve of **BChE-FP** catalyzed by BChE (0.02 U/mL) in phosphate buffer (100 mM, pH 7.0) with fluorometric method. (B) Dixon plot of inhibitory kinetics of Tacrine with **BChE-FP** (5 μM, 10 μM) as the substrate.

catalized hydrolysis for **BChE-FP** is muchhigher than that of other hydrolases and proteins, indicating that **BChE-FP** is particularly selective toward BChE. Most importantly, **BChE-FP** displayed over 14-fold better specificity to BChE compared to AChE, and the AChE mediated-hydrolysis of **BChE-FP** was comparable to the spontaneous hydrolysis that could be neglected. In addition, the molecular docking simulation revealed that the proximity of Ser-198 to the carbonyl group of **BChE-FP** was about 4.3 Å in BChE active site, whereas the proximity of Ser-203 to the carbonyl group of **BChE-FP** was about 7.4 Å in AChE active site (Fig. S35). Hence, the binding of **BChE-FP** in BChE active site is much more favourable to the Ser-triggered nucleophilic attack than that in AChE active site, which provides plausible evidence for the superior specificity to BChE. To the best of our knowledge, **BChE-FP** is the first selective probe that can discriminate BChE from AChE.

To further elucidate the applicability of **BChE-FP** as a substrate for evaluation of BChE activity, the kinetic properties of BChE-catalyzed hydrolysis of **BChE-FP** were investigated. According to the measurement of the FI change at the emission of 515 nm, the initial reaction rates for the enzymatic hydrolysis of **BChE-FP** were obtained at various concentrations of **BChE-FP** (0-50 μM). As anticipated, the plot of V versus S obeyed the Michaelis–Menten equation (shown in Fig. 5A). On the basis of the Michaelis–Menten curves, the Michaelis constant (K_m) and the catalytic rate constant (k_{cat}) of BChE for **BChE-FP** were determined to be 3.01 ± 0.32 μM and 104.75 ± 12.16 min^{-1}, respectively. Thus, the catalytic efficiency (k_{cat}/K_m) of BChE in processing **BChE-FP** is about 34.80 μM•min^{-1}. In this study, we also tested the K_m (308.07 ± 6.47 μM) and k_{cat} (20095 ± 143.65 min^{-1}) of BChE against ATC with Ellman's method under the same condition. Based on the kinetic parameters, the binding affinity of BChE-FP with BChE is ~100-fold higher than that of ATC, while the catalytic constant for **BChE-FP** is ~190-fold lower than that of ATC. Taken together, the overall catalytic efficiency of BChE against **BChE-FP** (~34.80 $μM^{-1}$• min^{-1}) is quite comparable to that of ATC (~65.24 $μM^{-1}$• min^{-1}). These kinetic analyses imply that **BChE-FP** can be a suitable substrate for BChE activity assessment.

Next, the BChE inhibition study was carried out using the turn-on fluorogenic system with **BChE-FP**. Tacrine, a well-known inhibitor of cholinesterases, was selected as the reference. All the reaction systems were incubated in the 96-well plates at 30 °C and the fluorescence at 515 nm was continually monitored for 5 min. The FI of the samples composed of **BChE-FP** (10 μM), BChE (0.02 U/mL) and different amounts of tacrine (0.1 to 20 μM) were monitored in different reaction time points. As expected, the FI linearly increased by prolonging the reaction time, but the speed of the fluorescence enhancement reduced gradually when the concentration of tacrine increased (see Fig. S36). The Dixon plot for inhibitory kinetics of tacrine was then obtained from the above time-dependent profile (Fig 5B). The average values of the K_i of tacrine toward BChE were estimated to be 10.69 ± 3.27 nM by using our assay, which is close to that obtained with Ellman's method (8.70 ± 0.17 nM).[10] The above results demonstrated that **BChE-FP** has a great potential to be used as a reliable fluorogenic substrate for discovering BChE inhibitors in moderate conditions.

To disclose the sensing capability of **BChE-FP** in cellular environment, we further applied **BChE-FP** to image the endogenous BChE in PANC-1 cells. We checked the cytotoxicity of **BChE-FP** against this PANC-1 cells and found no significant cytotoxicity up to 50 μM for 24 hours (See Fig S37). Furthermore no fluorescence was observed without any treatment (data not shown). After incubating the cells with **BChE-FP** (20 μM) for 20 min, the bright green fluorescence appeared, and the co-staining with Hoechst 33342 revealed that the endogenous BChE was located in the cytoplasm of PANC-1 cells (Fig. 6A-6D). Intriguingly, once the cells were pre-treated with the well- known inhibitor tacrine (50 μM) before the addition of the probe **BChE-FP** (20 μM), the green fluorescence signal was significantly diminished (Fig. 6E-6H). In addition, we conducted the flow cytometry analysis of PANC-1 cells exposed to different concentrations of **BChE-FP** (0 μM to 20 μM) to obtain the quantification result of imaging without and with the preincubation of cholinesterase inhibitor. It turned out that tacrine had similar inhibition potency against BChE and AChE, while the donepezil was a specific AChE inhibitor. Based on the original data (See Fig S38), it was easily observed that the fluorescence signal enhanced with the increased concentration of **BChE-FP** without addition of any inhibitor. More interestingly, the preincubation with tacrine significantly decreases the FI, whereas the FI of the same cells

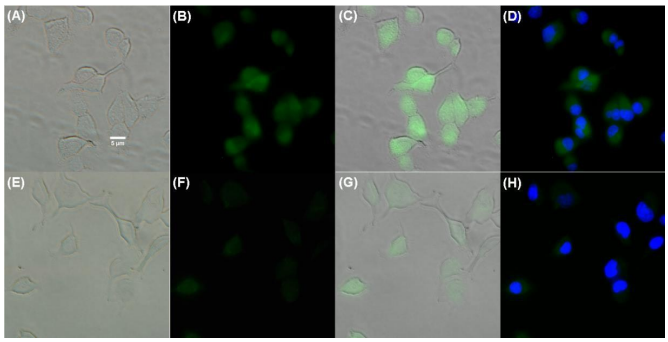

Fig. 6 Fluorescence images of **BChE-FP** (20 μM) in living PANC-1 cells treated without and with 50 μM tacrine. In top panel, the images of cells treated with **BChE-FP** (20 μM) and Hoechst 33342 (10 μM) in bright field (A), the dark fields (B and D), merge of A and B (C). In bottom panel, the images of cells treated with tacrine (50 μM) prior to the addition of **BChE-FP** (20 μM) for 20 min and Hoechst 33342 (10 μM) for 5 min in bright field (E), the dark fields (F and H), merge of E and F (G).

treated with Donepezil (a specific AChE inhibitor) did not exhibit remarkable FI reduction. These results indicated the promising applicability of probe **BChE-FP** in the development of cell-based assay for endogenous BChE detection and discrimination of BChE from AChE.

In conclusion, a small-molecular **BChE-FP**, acted as a specific fluorogenic substrate for BChE, was identified by structure difference-oriented design and stepwise optimization. **BChE-FP** showed very low background and exhibited remarkable bright fluorescence upon the catalysis of BChE. In addition, BChE showed about 100-fold higher binding affinity against **BChE-FP** than the most widely used substrate ATC, and the overall catalytical efficiency for **BChE-FP** was comparable to that of ATC. It also exhibited >14-fold specificity for BChE over AChE, producing 275-fold higher fluorescence enhancement upon the catalysis by BChE. In all, **BChE-FP** is a typical BChE-specific probe that can discriminate BChE from AChE. Additionally, the **BChE-FP** based turn-on fluorescent assay was established for evaluating BChE activity in aqueous solution and in living cells, and subsequently applied in BChE inhibitors screening and characterization. It was also found that **BChE-FP** could detect the endogenous BChE in living cells. The current study demonstrated that the **BChE-FP** had tremendous potential in future high-throughput studies in drug discovery and clinical diagnosis of BChE-associated diseases. Furthermore, this study implies that the structure difference-oriented design strategy offers a new approach that can be generally applied to designing protein isoform-specific probes.

We acknowledge the financial support from National Natural Science Foundation of China (21332004, 21672079 and 21372094) and the Science and Technology Planning Project of Guangdong Province of China (2015A010107002).

Notes and references

1. (a) O. Lockridge, *Pharmacol. Ther.*, 2014, **148**, 34; (b) A. Tripathi and U. C. Srivastava, *Ann. Neurol.*, 2008, **15**, 106; (c) G. Inacio Lunkes, F. Stefanello, D. Sausen Lunkes, V. Maria Morsch, M. R. Schetinger and J. F. Goncalves, *Diabetes Res. Clin. Pract.*, 2006, **72**, 28; (d) C. G. Ballard, N. H. Greig, A. L. Guillozet-Bongaarts, A. Enz and S. Darvesh, *Curr. Alzheimer Res.*, 2005, **2**, 307.
2. (a) N. G. Vallianou, A. A. Evangelopoulos, V. Bountziouka, M. S. Bonou, C. Katsagoni, E. D. Vogiatzakis, P. C. Avgerinos, J. Barbetseas and D. B. Panagiotakos, *J. Cardiovascul. Med.*, 2014, **15**, 377; (b) M. Stojanov, A. Stefanovic, G. Dzingalasevic, S. Mandic-Radic and M. Prostran, *Clin. Biochem.*, 2011, **44**, 623: (c) A. Contestabile, *Behav. Brain Res.*, 2011, **221**, 334; (d) A. Tasker, C. G. Ballard, C. Joachim, D. R. Warden, E. J. Okello, R. H. Perry, N. Khan, A. D. Smith, D. J. Lehmann and E. K. Perry, *Neurosci. Lett.*, 2008, **442**, 297.
3 (a) M. Di Carlo, D. Giacomazza and P. L. San Biagio, *J. Phys. Condens. Matter.*, 2012, **24**, 244102; (b) F. Zheng and C. G. Zhan, *Org. Biomol. Chem.*, 2008, **6**, 836; (c) D. Gao, H. Cho, W. Yang, Y. Pan, G. Yang, H. H. Tai and C. G. Zhan, *Angew. Chem. Int. Ed. Engl.*, 2006, **45**, 653; (d) C. G. Zhan, F. Zheng and D. W. Landry, *J. Am. Chem. Soc.*, 2003, **125**, 2462; (e) Y. Ashani, *Drug Dev. Res.*, 2000, **50**, 298.
4. (a) S. Z. Liao, W. T. Han, H. Z. Ding, D. X. Xie, H. Tan, S. Y. Yang, Z. Y. Wu, G. L. Shen and R. Q. Yu, *Anal. Chem.*, 2013, **85**, 4968; (b) O. Holas, K. Musilek, M. Pohanka and K. Kuca, *Expert Opin. Drug Discov.*, 2012, **7**, 1207; (c) Y. Miao, N. He and J. J. Zhu, *Chem. Rev.*, 2010, **110**, 5216; (d) L. H. Peng, G. X. Zhang, D. Q. Zhang, J. F. Xiang, R. Zhao, Y. L. Wang and D. B. Zhu, *Org. Lett.*, 2009, **11**, 4014; (e) G. L. Ellman, K. D. Courtney, V. Andres, Jr. and R. M. Feather-Stone, *Biochem. Pharmacol.*, 1961, **7**, 88; (f) K. Cui, Z. Chen, Z. Wang, G. Zhang and D. Zhang, *Analyst*, 2011, **136**, 191; (g) G. Zhou, F. Wang, H. Wang, S. Kambam, X. Chen and J. Yoon, *ACS Appl. Mater. Interfaces*, 2013, **5**, 3275; (h) S. Liao, W. Han, H. Ding, D. Xie, H. Tan, S. Yang, Z. Wu, G. Shen and R. Yu, *Anal. Chem.*, 2013, **85**, 4968; (i) D. Liao, J. Chen, H. Zhou, Y. Wang, Y. Li and C. Yu, *Anal. Chem.*, 2013, **85**, 2667; (j) L. M. Yang, J. Han, W. Liu, J. Q. Li and L. Jiang, *Anal. Chem.*, 2015, **87**, 5270; (k) N. Xia, Q. Wang and L. Liu, *Sensors*, 2015, **15**, 499.
5. (a) S. Kang, S. Lee, W. Yang, J. Seo and M. S. Han, *Org. Biomol. Chem.* , 2016, **14**, 8815; (b) J. Chen, D. Liao, Y. Wang, H. Zhou, W. Li and C. Yu, *Org. Lett.*, 2013, **15**, 2132.
6. S. Chao, E. Krejci, V. Bernard, J. Leroy, L. Jean and P. Y. Renard, *Chem. Commun.*, 2016, **52**, 11599.
7. (a) C. G. Zhan, F. Zheng, D. W. Landry, *J. Am. Chem. Soc.* 2003, **125**, 2462; (b) X. Chen, L. Fang, J. Liu, C. G. Zhan, *J. Phys. Chem. B* 2011, **115**, 1315; (c) S. Hou, L. Xue, W. Yang, L. Fang, F. Zheng, C. G. Zhan, *Org. Biomol. Chem.* 2013, **11**, 7477.
8. (a) Y. Nicolet, O. Lockridge, P. Masson, J. C. Fontecilla-Camps, F. Nachon, *J. Biol. Chem.* 2003, **278**, 41141; (b) G. Kryger, M. Harel, K. Giles, L. Toker, B. Velan, A. Lazar, C. Kronman, D. Barak, N. Ariel, A. Shafferman, I. Silman, J. L. Sussman, *Acta. Crystallogr. D Biol. Crystallogr.* 2000, **56**, 1385; (C) L. Fang, Y. Pan, J. L. Muzyka, C. G. Zhan, *J. Phys. Chem. B* 2011, **115**, 8797.
9. (a) L. Feng, Z. M. Liu, L. Xu, X. Lv, J. Ning, J. Hou, G. B. Ge, J. N. Cui and L. Yang, *Chem. Commun.*, 2014, **50**, 14519; (b) L. Tian, Y. Yang, L. M. Wysocki, A. C. Arnold, A. Hu, B. Ravichandran, S. M. Sternson, L. L. Looger and L. D. Lavis, *Proc. Natl. Acad. Sci. U. S. A.*, 2012, **109**, 4756.
10. (a) Q. Sun, D. Y. Peng, S. G. Yang, X. L. Zhu, W. C. Yang, G. F. Yang, *Bioorg. Med. Chem.* 2014, **22**, 4784.; (b) D. Y. Peng, Q. Sun, X. L. Zhu, H. Y. Lin, Q. Chen, N. X. Yu, W. C. Yang, G. F. Yang, *Bioorg. Med. Chem.* 2012, **20**, 6739.